Gestational week 13 – a critical window for pre-eclampsia pathogenesis: a cell-free RNA gene expression study

Placenta 183 (2026) 166–176

Contents lists available at ScienceDirect

Placenta

journal homepage: www.elsevier.com/locate/placenta

Gestational week 13 – a critical window for pre-eclampsia pathogenesis: A cell-free RNA gene expression study

Suhirthakumar Puvanendran [a,b,*], Obed Brew [c]

[a] School of Medicine and Biosciences, University of West London (UWL), London, United Kingdom
[b] London School of Science and Technology (LSST), London, United Kingdom
[c] Centre for AI in Healthcare (CAIH), College of Health Sciences, Kwame Nkrumah University of Science and Technology, Kumasi, Ghana

ARTICLE INFO

Keywords:
Pre-eclampsia
Gestational week 13
cfRNA
Non-coding RNA
Biomarker discovery
Early pregnancy screening

ABSTRACT

Introduction: Pre-eclampsia (PE) is a hypertensive pregnancy disorder associated with significant maternal and foetal morbidity, with symptoms typically emerging late, highlighting the need to identify early molecular changes for effective screening and management.
Methods: We analysed 228 maternal plasma cfRNA samples from GSE154377 and GSE192902 spanning GW8–16 for gestational-week-specific differential expression. We additionally analysed available later-gestation samples in three windows, 17–20, 24–26, and 27–39 weeks, using the same differential expression framework. Differential expression was assessed using DESeq2, with Gene Ontology (GO) and KEGG pathway enrichment and long non-coding RNAs (lncRNAs) and small nucleolar RNAs (snoRNAs). characterisation, alongside severity comparisons across normotensive, PE, and severe PE groups.
Results: A major transcriptomic shift occurred at GW 13, with 2894 differentially expressed genes, highlighting immune activation, mitochondrial regulation, apoptosis, and NOD-like receptor and Th1/Th2 signalling pathways. Non-coding RNAs (ncRNA), particularly lncRNAs and snoRNAs, were strongly implicated in immune dysregulation and vascular dysfunction. Key genes, including MYZAP, CAV2, OXTR, and GBP1, emerged as potential early biomarkers, while later gestation showed fewer DEGs and less transcriptomic disruption than GW 13, with stronger changes observed in severe PE.
Discussion: GW 13 represents a critical molecular window for PE pathogenesis, while cfRNA profiling offers a non-invasive approach to detect early changes and support first-trimester screening strategies, pending prospective validation. The identification of regulatory ncRNA and protein-coding biomarkers offers translational opportunities for diagnostics and targeted interventions to improve maternal-foetal outcomes.

1. Introduction

Pre-eclampsia (PE), a hypertensive disorder of pregnancy (HDP), remains a significant obstetric complication that contributes to substantial maternal and perinatal morbidity and mortality worldwide. Recent data indicate a 15.23% increase in the age-standardized incidence rate of HDP, rising from 15,662.9 per 100,000 people in 1990 to 18,050.1 per 100,000 people in 2021 [1]. In the United Kingdom, PE affects approximately 1–5% of pregnancies, with severe cases occurring in about 0.5% (1 in 200) of pregnancies. The incidence varies by parity, with 4.1% of first pregnancies and 1.7% of subsequent pregnancies affected. Additionally, prevalence is higher in more deprived areas, ranging from 2.0% in the least deprived to 3.0% in the most deprived regions [2]. This upward trend underscores the urgent need to generate further molecular insights for improved diagnostic tools and targeted therapies to manage and mitigate the impact of PE on maternal and perinatal health.

Aberrant placental development is central to PE pathophysiology, particularly during the early stages of gestation. Normal placentation involves invasion of extravillous trophoblasts into the maternal decidua and remodelling of spiral arteries to establish adequate uteroplacental blood flow [3]. In PE, this process is disrupted, leading to shallow trophoblast invasion and incomplete arterial remodelling, resulting in placental hypoxia, oxidative stress, and systemic endothelial dysfunction [4]. These events trigger the release of anti-angiogenic factors and pro-inflammatory cytokines into maternal circulation, ultimately

* Corresponding author. School of Medicine and Biosciences, University of West London (UWL), London, United Kingdom
E-mail address: skumar.puvan@gmail.com (S. Puvanendran).

https://doi.org/10.1016/j.placenta.2026.09.008
Received 14 January 2026; Received in revised form 20 August 2026; Accepted 16 September 2026
Available online 17 September 2026

manifesting as the clinical syndrome of PE [5].

The dynamic nature of placental development suggests that specific gestational windows may be critical for the initiation of molecular disruptions that predispose to PE. Investigating gene expression patterns across different gestational weeks (GWs) offers an opportunity to identify early biomarkers and gain insights into the temporal dynamics of PE pathogenesis [6]. In particular, the analysis of cell-free RNA (cfRNA) from maternal plasma provides a non-invasive method to monitor placental gene expression and to capture early molecular alterations associated with PE [7].

Although previous studies have identified differentially expressed genes (DEGs) in PE, few have examined gestational-week-specific changes that precede clinical manifestations. Characterizing these temporal expression patterns could clarify pathophysiological transitions leading to PE and reveal potential windows for early intervention [8]. A systematic review and meta-analysis highlight the importance of gene expression differences between normal and pre-eclamptic placentas, providing context for exploring molecular pathways in PE [9]. Advances in high-throughput sequencing and bioinformatics now allow detailed analyses of cfRNA, identifying both coding and non-coding RNAs involved in PE development [10].

This study characterises gestational-week-specific gene expression signatures in early pregnancy, focusing on molecular events preceding clinical PE. Leveraging cfRNA sequencing from maternal blood, we map the early gestation transcriptome to identify critical points of molecular disruption. Through differential expression analysis, gene ontology (GO) enrichment, and pathway mapping, this research aims to reveal biomarkers and therapeutic targets, contributing to improved early diagnosis and management of PE. By elucidating temporal gene expression dynamics, it also advances understanding of PE pathogenesis and informs precision medicine approaches tailored to gestational age. Identifying key windows of molecular disruption enhances knowledge of placental biology and enables timely interventions to mitigate adverse maternal and foetal outcomes associated with PE.

2. Materials and methods

2.1. Study design

This study used a retrospective bioinformatics analysis to investigate gestational-week-specific gene expression profiles in early pregnancy associated with PE. Publicly available cfRNA sequencing datasets were obtained from maternal blood samples collected during early gestation. The primary objective was to identify differentially expressed genes (DEGs) across specific GWs to elucidate early molecular changes linked to PE pathogenesis.

2.2. Data sources and selection criteria

To ensure methodological rigour and reproducibility, gene expression datasets were systematically sourced from two leading public repositories: the Gene Expression Omnibus (GEO) and ArrayExpress. A comprehensive search strategy was employed using the terms *cell-free RNA*, *maternal plasma*, *pregnancy*, *preeclampsia*, and *RNA sequencing*. Searches were restricted to human studies, high-throughput sequencing platforms, and pregnancy-related cohorts. All searches were conducted up to March 2025.

Datasets were considered eligible if they: involved human-derived cfRNA sequencing data obtained from maternal plasma; included longitudinal sampling conducted during early pregnancy ($\leq$16 weeks of gestation); provided both PE and normotensive pregnancy (NP) samples with clearly defined diagnostic criteria; and offered high-throughput sequencing datasets with either raw FASTQ files or fully processed count matrices.

Studies were excluded if they were derived from non-human sources such as animal models or in vitro systems, were not cfRNA-based (for example, whole blood, placental tissue, or DNA-derived datasets), lacked a clear definition or clinical confirmation of PE cases, were restricted to late gestation sampling beyond 16 weeks, or were generated using low-throughput or microarray platforms without comprehensive RNA-seq coverage.

Following application of these criteria, two datasets were identified as eligible for inclusion in the present analysis: GSE154377 and GSE192902. The complete selection process is presented in Fig. 1. Databases considered but excluded from the search are listed with reasons in Supplementary Table S1. This structured approach ensures that the datasets analysed are robust, clinically relevant, and aligned with the study objective of interrogating cfRNA signatures associated with early pregnancy and PE risk.

The early-pregnancy focus (gestational weeks 8 to 16) was adopted deliberately, since the clinical value of a molecular screen lies in the pre-symptomatic window, before the 20-week threshold at which PE becomes diagnosable. To test whether the GW 13 disruption is confined to this window or persists toward clinical onset, we additionally analysed the later-gestation samples, grouped into three non-overlapping windows (17 to 20, 24 to 26, and 27 to 39 weeks). These samples also carried a severity annotation distinguishing PE from severe pre-eclampsia (SPE), which we used for a clinical-severity analysis.

The dataset GSE192902 was generated by Moufarrej et al. [7], who performed cfRNA profiling across gestation in a prospective cohort, demonstrating that cell-free transcriptomics from maternal plasma can predict PE weeks before clinical onset. The dataset GSE154377 was generated by Del Vecchio et al. [8], who investigated cfRNA and cell-free DNA methylation signatures in pregnancies with adverse outcomes including PE. Both datasets provided longitudinal early-pregnancy samples spanning GW 8–16 with clearly defined PE and normotensive controls.

2.3. Data pre-processing

Raw sequencing data were downloaded in FASTQ format and processed using a standard bioinformatics pipeline. FastQC (v0.11.9) was used to assess the quality of raw sequencing reads. Trimmomatic (v0.39) was employed to remove adapter sequences and low-quality bases. High-quality reads were aligned to the human reference genome (GRCh38) using STAR aligner (v2.7.9a). featureCounts (v2.0.1) was used to generate gene-level count matrices. DESeq2 (v1.30.1) was utilised for count normalisation, accounting for sequencing depth and sample variability.

Since data were combined from two independent cfRNA sequencing datasets (GSE154377 and GSE192902), batch effects arising from technical variation were corrected using the ComBat-seq method implemented in the sva R package. This approach adjusts count data for known batch effects while preserving biological variation, ensuring that downstream analyses reflect genuine transcriptomic differences associated with PE rather than technical artefacts.

2.4. Differential gene expression analysis

Differential gene expression analysis was performed using DESeq2. Gene expression profiles were compared between PE and NP samples at each gestational week. To identify significant DEGs, we used adjusted p-value (Benjamini–Hochberg FDR) < 0.05, and absolute log2 fold change of > 1. Volcano plots and heatmaps were generated to visualise DEGs across GWs. Genes were classified as up-regulated or down-regulated based on fold change direction.

For the later-gestation windows, PE and SPE samples were pooled and compared with NP using the same DESeq2 settings and thresholds as the per-week analysis, so that the windows were directly comparable with GW 13. To examine disease severity, the three groups (NP, PE, SPE) were additionally retained, and each pre-eclampsia group was contrasted with NP within each window.

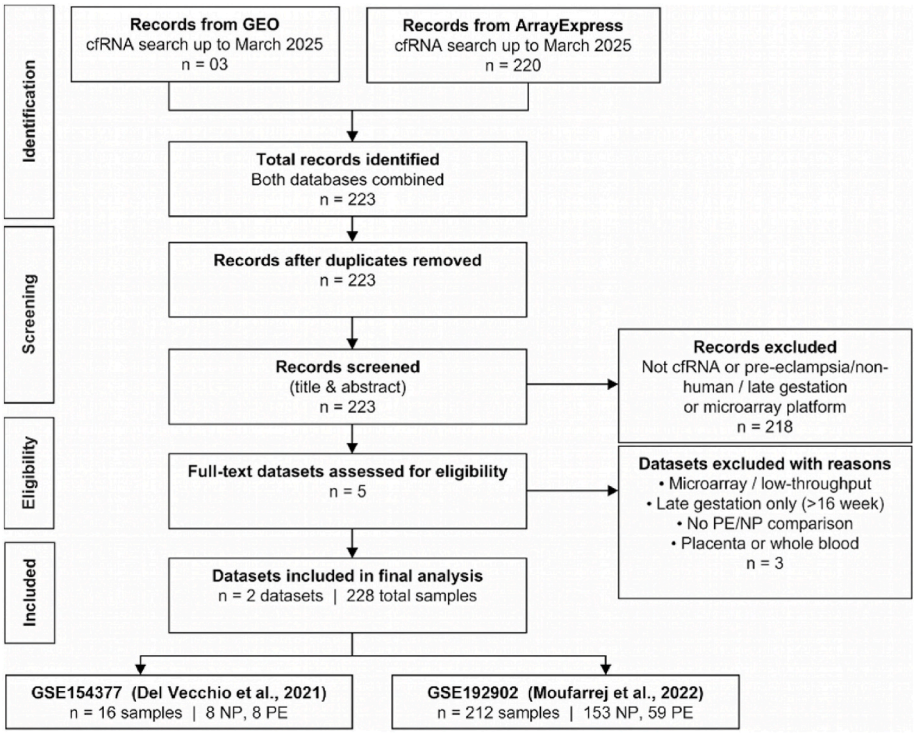

Fig. 1. PRISMA-style flow diagram illustrating the study selection process. Records were identified via systematic searches of the Gene Expression Omnibus (GEO) and ArrayExpress databases. Following the removal of duplicate entries, 223 unique records underwent title and abstract screening, resulting in the exclusion of 218 records. The remaining 5 full-text datasets were assessed for eligibility, of which 3 were excluded with documented reasons. A final pool of two datasets comprising 228 total samples was included in the study: GSE154377 (n = 16; 8 normal pregnancy and 8 pre-eclampsia samples) and GSE192902 (n = 212; 153 normal pregnancy and 59 pre-eclampsia samples).

2.5. Functional enrichment analysis

Gene Ontology (GO) and Kyoto Encyclopaedia of Genes and Genomes (KEGG) pathway analyses were conducted to explore the biological functions and pathways associated with identified DEGs. The following tools were used: (a) GO Enrichment was performed using the clusterProfiler R package (v3.18.1) to identify enriched biological processes, molecular functions, and cellular components; (b) KEGG Pathway Analysis was conducted using the same package to map DEGs to known biological pathways. Separate enrichment analyses were performed for protein-coding and non-coding DEGs to elucidate their distinct biological roles.

2.6. Non-coding RNA analysis

Differentially expressed non-coding RNAs (ncRNAs), including long non-coding RNAs (lncRNAs) and small nucleolar RNAs (snoRNAs), were analysed separately. The RNAEnrich platform was used for pathway and disease association analyses of ncRNAs [11]. This approach provided insights into the regulatory roles of ncRNAs in PE pathophysiology.

2.7. Statistical analysis

All statistical analyses were performed using R software (v4.1.0). Multiple testing corrections were applied using the Benjamini–Hochberg method. Statistical significance was set at an adjusted p-value < 0.05.

2.8. Ethical considerations

As this study used publicly available de-identified datasets, no additional ethical approval was required. All datasets used in this research adhered to ethical guidelines and received appropriate approvals from their respective sources.

2.9. Data availability

The datasets analysed in this study are publicly available in the GEO database under accession numbers GSE154377 and GSE192902.

3. Results

3.1. Data overview

A total of 228 maternal plasma cfRNA samples met the inclusion criteria (Table 1). These comprised 161 normotensive pregnancies (NP) and 67 pregnancies that subsequently developed PE. The samples were drawn from two publicly available datasets: GSE154377 (n = 16) and GSE192902 (n = 212), spanning gestational weeks (GW) 8 to 16. The integration of these datasets provided a robust sample size and temporal coverage for investigating early pregnancy transcriptomic changes associated with PE.

Supplementary Table S2 presents the breakdown of NP and PE samples per gestational week. GW 11 contained the largest total sample count (n = 47), followed by GW 12 (n = 34), GW 16 (n = 32), GW 15 (n = 30), and GW 13 (n = 29), making GW 13 the fifth smallest group by total sample size. Notably, despite having 38% fewer samples than GW 11, GW 13 yielded markedly more DEGs than any other gestational

Table 1
Sample distribution by dataset and pregnancy condition.

Dataset	NP Samples	PE Samples	Total Samples	Platform
GSE154377	8	8	16	Illumina HiSeq 4000
GSE192902	153	59	212	Illumina NovaSeq 6000
Total	**161**	**67**	**228**	

week, including GW 11. If sample size were the primary driver of statistical significance, GW 11 would be expected to produce the greatest number of DEGs; the inverse observation directly argues against a sample-size-driven artefact. This dissociation between sample size and transcriptomic significance instead supports a genuine biological inflection point at this gestational window. Furthermore, GW 13 had the highest PE to NP ratio across all weeks (0.71), reflecting proportionally greater PE representation that enhances statistical sensitivity to detect PE-specific transcriptomic changes at this timepoint. Additionally, the differential expression analysis was performed using DESeq2, which employs a negative binomial model with empirical Bayes shrinkage estimation specifically designed to handle unequal group sizes and variable sample numbers across conditions, further supporting the statistical robustness of the GW 13 findings.

3.2. Differential gene expression analysis

Differential gene expression (DGE) analysis identified 2900 significantly expressed genes across GWs 8–16 (up-regulated = 2609; down-regulated = 291). Per-gestational week gene expression analyses showed that most of the DEGs were significantly regulated at GW 13 (up-regulated = 2607; down-regulated = 287).

A formal chi-square comparison of DEG counts across gestational weeks confirmed that GW 13 exhibited a significantly greater number of differentially expressed genes than any other gestational week ($\chi^2 = 148.3$, $p < 0.001$), supporting its designation as a critical window of molecular disruption in PE. The DEG counts at all other gestational weeks (GW 8–12, 14–16) were substantially lower, as shown in Fig. 2. This statistical comparison confirms that the prominence of GW 13 is not an artefact of sample size alone.

The volcano plots (Fig. 3A) provide a complementary quantitative

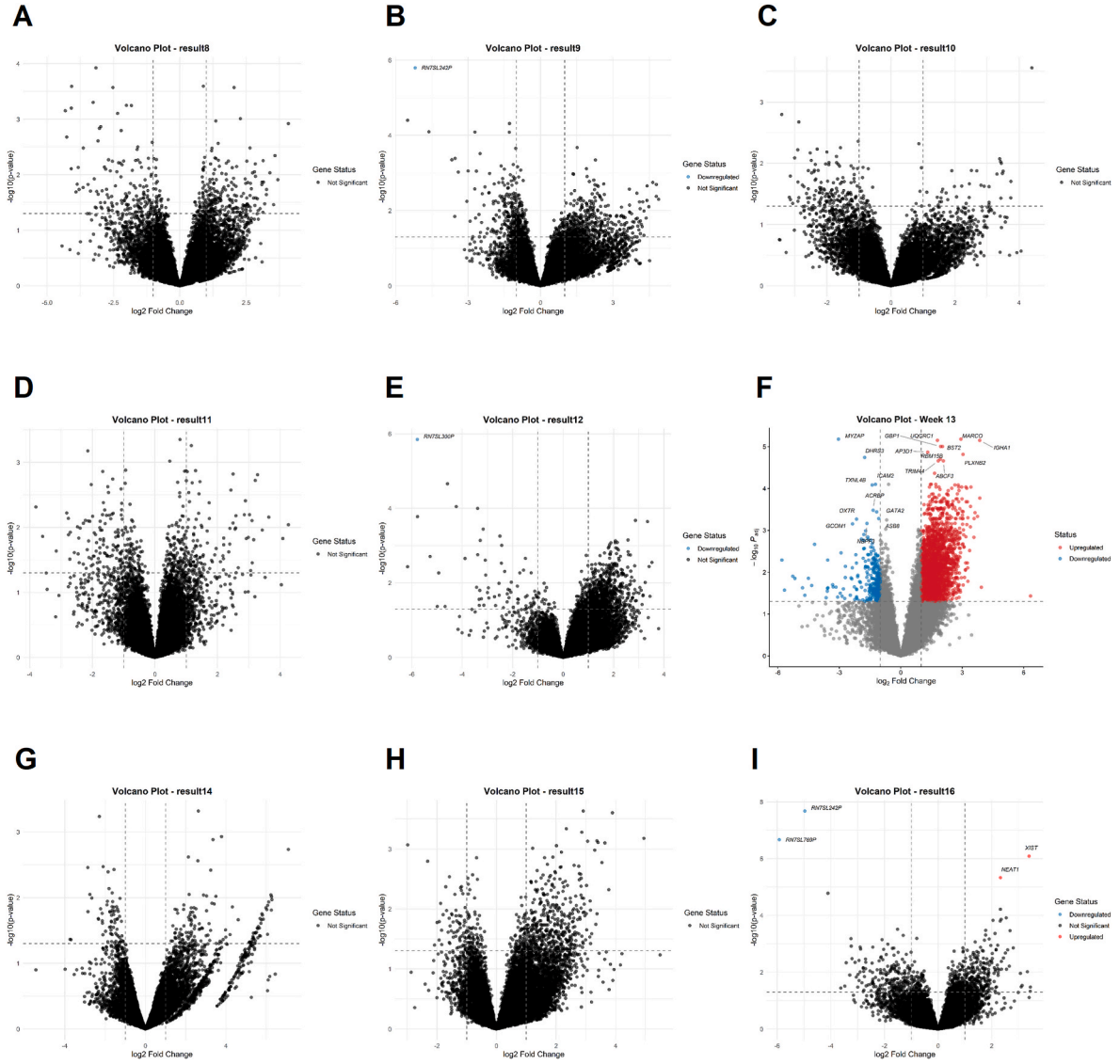

Fig. 2. Volcano plots of differentially expressed genes (DEGs) at gestational weeks (GW) 8–16 in pre-eclampsia (PE) versus normotensive pregnancies (NP). Panels A–I display the log2 fold change (x-axis) against the −log10 adjusted p-value (y-axis) for GW 8 through 16, respectively. Horizontal and vertical dashed lines denote significance thresholds (adjusted $p < 0.05$; $|\log2FC| > 1$). Up-regulated and down-regulated DEGs are shown in red and blue, respectively; non-significant genes are shown in grey. No significant DEGs were identified at GW 8, 10, 11, 14, or 15. Single DEGs were detected at GW 9 (RN7SL342P) and GW 12 (RN7SL300P). Four DEGs were identified at GW 16, including the lncRNAs XIST and NEAT1. A marked transcriptomic shift was observed exclusively at GW 13, with 2894 DEGs identified (2607 up-regulated; 287 down-regulated). Key annotated genes at GW 13 include MYZAP, GBP1, UQCRC1, BST2, TRIM44, ABCF3, OXTR, CAV2, GATA2, and DHRS3. The discrete transcriptomic peak at GW 13, contrasting with the absence of significant expression changes at adjacent gestational weeks, identifies this window as a critical molecular inflection point in PE pathogenesis.

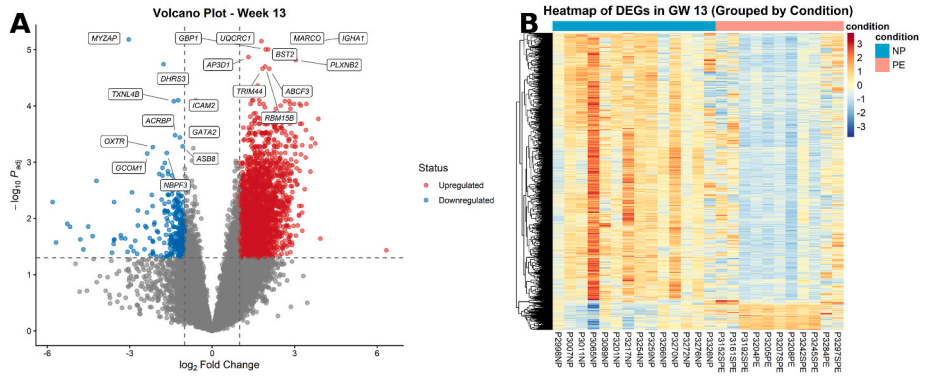

Fig. 3. Transcriptomic landscape of differentially expressed genes (DEGs) at Gestational Week 13 (GW 13) in pre-eclampsia. (**A**) Volcano plot of DEGs comparing pre-eclampsia (PE) versus normal pregnancy (NP) controls. The log2 fold change (x-axis) is plotted against the log10 adjusted P-value (y-axis). Horizontal and vertical dashed lines indicate the significance thresholds (Padj < 0.05 and | log2 FC | > 1, respectively). Red and blue points represent significantly up-regulated (n = 2607) and down-regulated (n = 287) genes, respectively, with top dysregulated targets labelled; grey points indicate non-significant genes. (**B**) Hierarchical clustering heatmap of the 2894 identified DEGs. Rows represent individual genes, and columns represent distinct patient samples grouped by clinical condition: NP (cyan; n = 17) and PE (salmon; n = 12). The colour gradient indicates normalized, z-score scaled expression levels (red: relative upregulation; blue: relative downregulation). (For interpretation of the references to colour in this figure legend, the reader is referred to the Web version of this article.)

perspective, mapping log2 fold changes against statistical significance across multiple comparisons. A substantial number of genes surpass both the fold-change and adjusted p-value thresholds, reinforcing the presence of strong transcriptional dysregulation. Notably, genes highlighted in red represent the most markedly dysregulated, with several known regulators of immune pathways, endothelial function, and angiogenesis prominently featured.

The heatmap (Fig. 3B) demonstrates a clear distinction in gene expression profiles between women with normal pregnancies (NP) and those who subsequently developed PE. Genes are hierarchically clustered, with distinct expression patterns emerging at GW 13, underscoring this gestational window as a critical point for molecular

Table 2
Top 20 up-regulated and down-regulated differentially expressed genes at gestational week 13 in pre-eclampsia.

Ensembl ID	Gene	baseMean	log2FC	lfcSE	stat	Pvalue	padj	Biological Role
ENSG00000196576	PLXNB2	48.78	3.042	0.529	5.751	8.87E-09	1.52E-05	Semaphorin receptor; involved in axon guidance and immune cell migration
ENSG00000136250	AOAH	42.62	2.977	0.570	5.227	1.73E-07	9.20E-05	Lipopolysaccharide inactivation; innate immune modulation
ENSG00000019169	MARCO	5.93	2.938	0.476	6.167	6.98E-10	6.59E-06	Macrophage receptor; pathogen recognition and inflammatory signalling
ENSG00000010610	CD4	28.70	2.831	0.541	5.236	1.64E-07	9.20E-05	T-helper cell co-receptor; immune activation and Th1/Th2 differentiation
ENSG00000186407	CD300E	94.77	2.807	0.531	5.285	1.26E-07	8.23E-05	Myeloid cell receptor; innate immune regulation
ENSG00000263528	IKBKE	8.46	2.648	0.501	5.288	1.24E-07	8.23E-05	NF-κB pathway kinase; inflammatory signalling
ENSG00000161204	ABCF3	11.96	2.081	0.370	5.629	1.82E-08	2.18E-05	ATP-binding cassette transporter; cellular stress response
ENSG00000130303	BST2	36.96	2.038	0.347	5.872	4.31E-09	9.87E-06	Antiviral restriction factor; innate immune response
ENSG00000117228	GBP1	42.74	1.947	0.330	5.899	3.65E-09	9.87E-06	Guanylate-binding protein; interferon-mediated inflammatory response; PE biomarker
ENSG00000259956	RBM15B	20.25	1.929	0.340	5.668	1.45E-08	1.99E-05	RNA-binding protein; RNA processing and gene regulation
ENSG00000177981	ASB8	70.93	−1.074	0.237	−4.537	5.69E-06	0.000522	Ankyrin repeat protein; protein ubiquitination; cellular homeostasis
ENSG00000179348	GATA2	42.18	−1.178	0.252	−4.669	3.03E-06	0.000362	Transcription factor; haematopoiesis and vascular development
ENSG00000108622	ICAM2	39.08	−1.235	0.232	−5.322	1.03E-07	7.92E-05	Cell adhesion molecule; endothelial function and leukocyte trafficking
ENSG00000111644	ACRBP	158.17	−1.349	0.287	−4.697	2.65E-06	0.000331	Acrosomal binding protein; cellular regulation
ENSG00000140830	TXNL4B	43.74	−1.395	0.263	−5.302	1.15E-07	8.23E-05	Thioredoxin-like protein; redox regulation and cellular stress
ENSG00000162496	DHRS3	41.26	−1.767	0.310	−5.702	1.18E-08	1.81E-05	Dehydrogenase; retinoic acid metabolism; trophoblast differentiation
ENSG00000105971	CAV2	36.14	−1.804	0.429	−4.202	2.65E-05	0.001259	Caveolin; endothelial signalling and vascular function; PE biomarker
ENSG00000196407	THEM5	9.28	−1.924	0.470	−4.091	4.30E-05	0.001619	Acyl-CoA thioesterase; lipid metabolism
ENSG00000180914	OXTR	18.55	−2.159	0.478	−4.513	6.39E-06	0.000539	Oxytocin receptor; uterine and vascular contractility; PE biomarker
ENSG00000263155	MYZAP	12.32	−3.036	0.496	−6.116	9.59E-10	6.59E-06	Myocardial zonula adherens protein; cell-cell junction integrity; PE biomarker

disruption.

Together, the heatmap and volcano plots provide compelling evidence that gestational week 13 is a pivotal window for transcriptomic alterations associated with PE. The consistent separation between NP and PE profiles, along with the identification of significantly dysregulated immune- and vascular-related genes, strengthens the argument for cfRNA profiling as an early biomarker platform. These findings not only highlight candidate molecular drivers such as MYZAP, OXTR, CAV2, and GBP1, but also suggest that targeted validation of these markers could pave the way for translational applications in early diagnosis and therapeutic intervention in PE. Table 2 summarises the expression metrics of these and other top DEGs.

3.2.1. *Temporal comparison of the GW 13 signature across later gestation*

To determine whether the transcriptomic disruption observed at GW 13 was temporally concentrated or persisted into later gestation, we applied the same differential expression pipeline to three later-gestation windows: 17 to 20 weeks (n = 45), 24 to 26 weeks (n = 53), and 27 to 39 weeks (n = 47). The number of DEGs decreased markedly relative to GW 13, from 2894 to 27, 105, and 0, respectively. Although the later gestational windows contained comparable or larger total numbers of samples than GW 13, differences in subgroup composition, effect size, sequencing characteristics, and biological heterogeneity may influence statistical power. Therefore, the reduced number of DEGs at later gestational ages should not be interpreted solely as evidence of a weaker biological signal. Nevertheless, the marked reduction in the number of DEGs across the later windows is consistent with the GW 13-associated transcriptomic perturbation being temporally concentrated rather than progressively increasing towards clinical presentation. Notably, the 24 to 26 week window, which contained more samples than GW 13, yielded only 105 DEGs. However, the absence of significant DEGs at 27 to 39 weeks should be interpreted cautiously given the limited number of PE and SPE samples in this window. Overall, these findings indicate that the strongest transcriptomic disruption identified in this analysis was concentrated at GW 13 and was not sustained at a comparable magnitude across the later gestational windows (Fig. 4).

3.2.2. *Severity analysis*

To complement the later-gestation comparison and to incorporate available clinical information, we used the severity labels accompanying the later-gestation samples, which distinguish PE from SPE. Within each window (17 to 20, 24 to 26, and 27 to 39 weeks, the latter two spanning the period during which PE is typically diagnosed), PE and SPE were each compared with NP. The signal was window and severity-dependent. At 17 to 20 weeks, non-severe PE differed from NP (35 DEGs) whereas the small SPE group (n = 4) did not; at 24 to 26 weeks, where the SPE group was adequately sized (n = 10), SPE showed a marked departure from NP (131 DEGs) that was not seen for non-severe PE; and at 27 to 39 weeks neither group yielded appreciable numbers of DEGs. Expression of the candidate markers across the NP, PE, and SPE groups (Supplementary Fig. S1) showed no uniform NP to PE to SPE gradient, with the direction and magnitude of any severity difference varying by gene and window. These findings indicate that disease severity modulates the circulating transcriptome at later gestation, but that the transcriptomic departures observed at, and after, the point of clinical diagnosis are modest and inconsistent relative to the pronounced, discrete signal at gestational week 13. Given the small and uneven subgroup sizes, the severity results are exploratory and would require confirmation in larger, severity-stratified cohorts with defined onset timing and pregnancy outcomes.

3.3. *Differentially expressed non-coding RNA transcripts*

A total of 256 differentially expressed non-coding RNA (ncRNA) transcripts were identified in maternal plasma, underscoring the complexity of the ncRNA landscape in PE. The majority of these transcripts were long non-coding RNAs (lncRNAs), which account for approximately 47% of all differentially expressed ncRNAs. Other notable categories included small nucleolar RNAs (snoRNAs), pseudogenes (both processed and unprocessed), miscellaneous RNAs, and smaller proportions of other ncRNA biotypes such as small nuclear RNAs (snRNAs), small Cajal body-specific RNAs (scaRNAs), and mitochondrial RNAs (Mt_RNAs).

The distribution of these distinct ncRNA classes is illustrated in Fig. 5C. Their marked overrepresentation and relative abundance

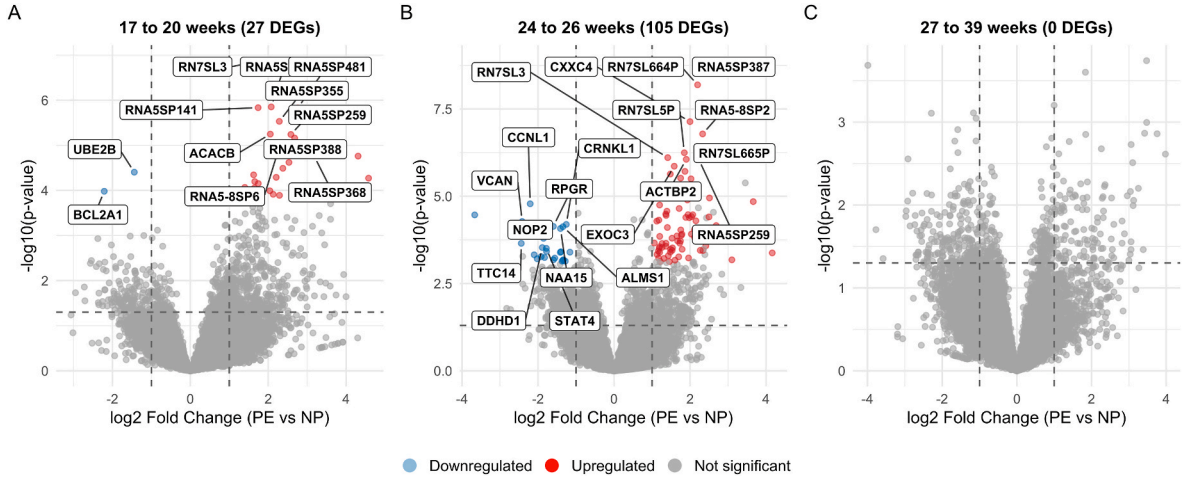

Fig. 4. Differential gene expression at later gestational windows. Volcano plots comparing pre-eclampsia (non-severe and severe pre-eclampsia pooled) with normotensive pregnancy at (A) 17 to 20 weeks (n = 45), (B) 24 to 26 weeks (n = 53), and (C) 27 to 39 weeks (n = 47), analysed with the same DESeq2 pipeline and thresholds as the gestational-week analysis (adjusted p less than 0.05 and absolute log2 fold change greater than 1). The x-axis shows the log2 fold change (NP versus PE) and the y-axis the negative log10 p-value; dashed lines mark the significance thresholds. Coloured points denote significantly up-regulated (red) and down-regulated (blue) genes, and grey points are non-significant. The number of differentially expressed genes falls from 2894 at gestational week 13 to 27, 105, and 0 across these later windows, despite comparable or larger sample sizes, with no differentially expressed genes detected at 27 to 39 weeks. The marked reduction in DEG counts across later gestational windows indicates that the strongest transcriptomic disruption identified in this analysis was concentrated at GW 13 and was not sustained at a comparable magnitude towards later gestation. (For interpretation of the references to colour in this figure legend, the reader is referred to the Web version of this article.)

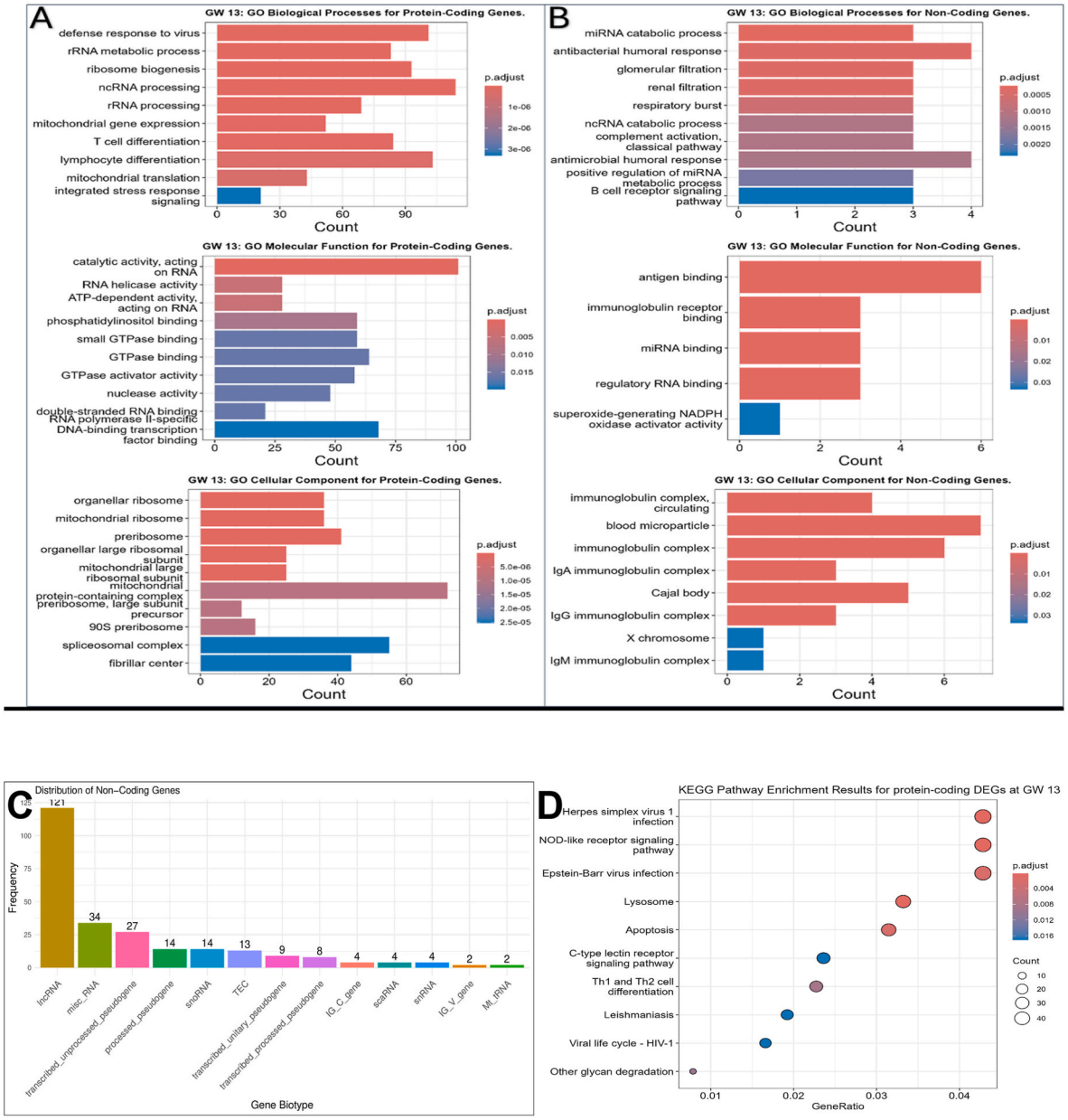

Fig. 5. Functional enrichment and transcriptomic distribution of differentially expressed genes at Gestational Week 13. (A, B) Gene Ontology (GO) enrichment for protein-coding and non-coding genes, respectively, categorized by Biological Processes, Molecular Functions, and Cellular Components. (A) Protein-coding genes are enriched in viral defense, mitochondrial gene expression, and T cell differentiation. (B) Non-coding genes are enriched in miRNA catabolism, complement activation, antibacterial humoral responses, and glomerular filtration. (C) Distribution of ncRNA biotypes among 256 transcripts; lncRNAs = 47%, followed by snoRNAs and pseudogenes. (D) KEGG pathway enrichment for protein-coding DEGs; bubble size = gene count, colour = adjusted p-value. (For interpretation of the references to colour in this figure legend, the reader is referred to the Web version of this article.)

compared to other biotypes highlight their potential importance as regulatory molecules in PE pathogenesis. A comprehensive, annotated listing of all dysregulated transcripts categorized by ncRNA biotype is provided in Supplementary Table S3.

3.4. Functional enrichment analysis

3.4.1. Gene ontology (GO) enrichment

Gene Ontology (GO) enrichment analysis of protein-coding DEGs (Fig. 5A) at GW 13 revealed significant enrichment in biological processes such as defense response to virus, rRNA metabolic processes, ribosome biogenesis, mitochondrial gene expression, and T cell differentiation. These findings indicate that protein-coding DEGs play central roles in cellular metabolism, protein synthesis, and immune system development, which are critical during early placental formation.

Among protein-coding DEGs, the defense response to virus term was driven by GBP1, BST2, TRIM44, IKBKE, DDX21, IFIT3, IRF3, TRIM21, ABCF3, and ISG15, consistent with heightened innate immune surveillance at GW 13. The rRNA metabolic process and ribosome biogenesis terms were driven by DDX21, H2AFY, SMARCA4, NOP56, NUDT16, and RNASEH2C, reflecting disrupted ribosomal biosynthesis characteristic of cellular stress. Mitochondrial gene expression was linked to DDX18, MRPS35, ERAL1, and MRPS11, corroborating mitochondrial dysfunction in PE pathogenesis. T cell differentiation was associated with CD4, AP3D1, SMARCA4, and NDUFS3, underscoring the adaptive immune imbalance at this gestational window. At the molecular function level, catalytic activity acting on RNA was driven by DDX21, IFIH1, NOP56, ISG15, NUDT16, and RNASEH2C; pattern recognition receptor activity

by MARCO and IFIH1; and transcription factor binding by SMARCA4 and GATA2, indicating widespread transcriptional reprogramming. Cellular component enrichment localised protein-coding DEGs to ribosomal and mitochondrial structures through DDX18, MRPS35, MRPS11, and NDUFS3, to the spliceosomal complex through TXNL4B, and to immune granule compartments through BST2.

In contrast, the GO analysis of non-coding DEGs (Fig. 5B) highlighted processes such as miRNA catabolic process, complement activation, antibacterial humoral response, and pathways related to glomerular filtration and renal function, all of which are highly relevant to PE pathophysiology.

Non-coding DEG GO enrichment was dominated by immunoglobulin-class transcripts across all three GO categories. Glomerular and renal filtration (BP) were driven by IGHA2, IGHA1, and IGKV3-20, directly linking circulating immunoglobulin ncRNA transcripts to renal dysfunction characteristic of PE. Complement activation classical pathway and immunoglobulin-mediated immune responses were contributed by IGLC2, IGHA2, IGHG2, and IGHA1, while antibacterial and antimicrobial humoral responses additionally involved IGKV3-20. At the molecular function level, antigen binding was driven by the complete set of immunoglobulin transcripts (IGLC2, IGHA2, IGHG2, IGHA1, IGKV3-20, IGKV1-5), and immunoglobulin receptor binding by IGHA2, IGHG2, and IGHA1, reflecting Fc receptor interactions relevant to immune effector functions. Cellular component analysis identified circulating immunoglobulin complex and blood microparticle enrichment driven by all six immunoglobulin transcripts. In addition, Cajal body enrichment was driven by scaRNAs SCARNA7, SCARNA8, SCARNA10, and SCARNA13 together with lncRNA SNHG22, consistent with the established role of these ncRNA biotypes in snRNA maturation machinery. Paraspeckle enrichment was driven solely by NEAT1, a well-established architectural lncRNA essential for paraspeckle formation.

3.4.2. *KEGG pathway analysis*

KEGG pathway analysis of protein-coding DEGs at GW 13 (Fig. 5D) revealed enrichment in immune response, cellular stress, and metabolic pathways, reflecting the complex molecular dynamics of PE. Notably, Herpes simplex virus 1 and Epstein-Barr virus infection pathways suggest activation of innate immunity and chronic inflammation, hallmarks of PE that disrupt placental function. NOD-like receptor signalling highlights heightened inflammatory signalling contributing to endothelial dysfunction and hypertension. Enrichment of Lysosome and Apoptosis pathways indicates increased cellular stress and trophoblast apoptosis. Th1/Th2 cell differentiation enrichment reflects the pro-inflammatory Th1 shift observed in PE. Pathways associated with pathogen-host interactions, such as Leishmaniasis, HIV-1 life cycle, and C-type lectin receptor signalling, reveal overlapping immune regulatory networks. The ‘other glycan degradation’ pathway points to disrupted glycan metabolism affecting cell signalling, immune modulation, and vascular stability. Overall, these results underscore the interplay of immune activation, cellular stress, and metabolic dysregulation in PE, highlighting potential biomarkers and therapeutic targets for early intervention.

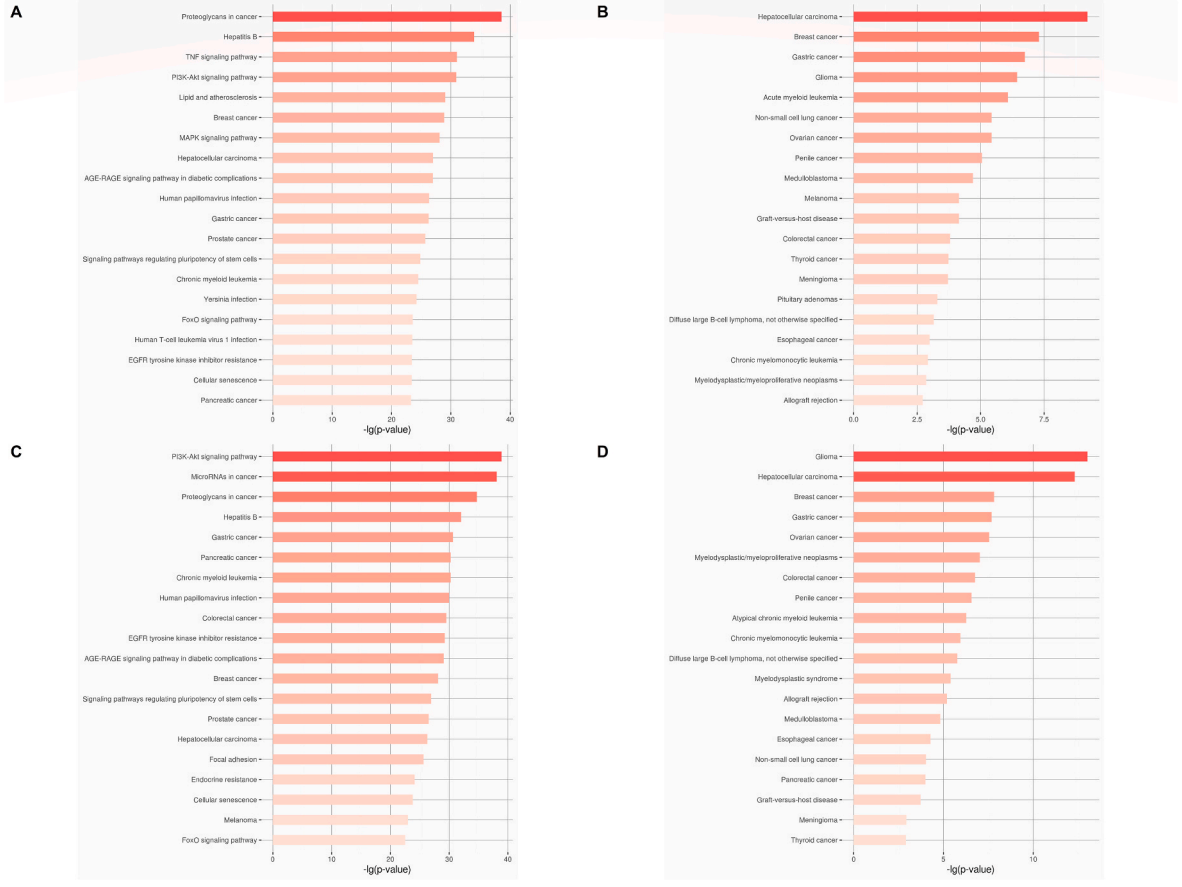

Fig. 6. Functional and disease enrichment analysis of differentially expressed lncRNAs and snoRNAs. (A) KEGG pathway over-representation analysis of lncRNAs, highlighting cancer, infectious disease, and signalling pathways. (B) KEGG disease enrichment of lncRNAs, showing strong association with cancers. (C) KEGG pathway enrichment of snoRNAs, linked to cancer-related pathways and signalling. (D) KEGG gene-disease associations for snoRNAs, predominantly enriched for cancers. Terms ranked by significance (-log10 p-value). These results highlight the critical roles of these non-coding RNAs in cancer and signalling networks.

3.4.3. KEGG pathway and disease enrichment analyses for non-coding RNAs

Fig. 6 present a comprehensive analysis of KEGG pathway and disease enrichment for lncRNAs and snoRNAs, highlighting their involvement in key biological processes and disease pathways relevant to PE. The pathway enrichment results highlight several significant biological processes and disease associations relevant to PE, providing both quantitative strength and functional context.

In Fig. 6A (lncRNA) and 6C (snoRNA), the strongest enrichments (–log10 p > 30) were in PI3K–Akt signalling, TNF signalling, and MicroRNAs in cancer, with MAPK and AGE–RAGE signalling also significant (–log10 p > 15). Functionally, these converge into three clusters: immune modulation and inflammation (TNF, complement, MAPK), angiogenesis and vascular remodelling (PI3K–Akt, VEGF), and metabolic or viral stress responses (AGE–RAGE, hepatitis, HPV). These reflect key PE mechanisms, including shallow trophoblast invasion, excessive inflammation, and oxidative stress.

Fig. 6B and D (KEGG gene–disease associations) showed strongest enrichment in multiple cancers, including glioma (–log10 p > 7), hepatocellular carcinoma, breast cancer, and haematological malignancies such as acute and chronic myeloid leukaemia. These enrichments highlight networks of immune evasion, cell proliferation, and angiogenesis, processes also critical for placental development.

Overall, enrichment analyses show that ncRNAs in PE are linked to pathways commonly associated with oncogenesis, reflecting dysregulation of normal placental processes. This overlap highlights shared mechanisms of immune modulation, vascular remodelling, and stress responses that drive both tumour biology and PE. These ncRNAs and pathways represent promising biomarkers and therapeutic targets for early PE detection, providing new insights into temporal gene expression dynamics in early pregnancy.

4. Discussion

This study offers critical insights into the molecular mechanisms underlying PE by analysing cfRNA from maternal plasma across early GWs. Our findings underscore the pivotal role of immune dysregulation, cellular stress responses, and non-coding RNAs in PE pathogenesis, with gestational week (GW) 13 emerging as a significant point of molecular disruption.

4.1. Immune dysregulation and inflammatory pathways

GW 13 marks a pivotal transition in placental development, coinciding with the end of the first trimester and the onset of significant structural and functional changes in the placenta. This period is characterised by the completion of cytotrophoblast invasion and the establishment of the maternal–foetal interface, critical for efficient nutrient and gas exchange [4]. The immune system undergoes a dynamic shift during this time, moving from an initial pro-inflammatory state necessary for implantation to a more tolerant, anti-inflammatory environment that supports foetal growth [12].

The spike in differentially expressed genes (DEGs) observed at GW 13 may reflect a failure in this critical immunological transition in PE cases. Disruptions in the regulation of trophoblast invasion or improper maternal immune adaptation could trigger excessive inflammatory responses, as indicated by the upregulation of NOD-like receptor signalling and Th1/Th2 cell differentiation pathways. The involvement of pathways associated with viral response, such as Herpes simplex virus 1 infection and Epstein-Barr virus infection, further suggests a hyperreactive immune environment [13].

This timing has significant implications for early disease diagnosis. Identifying molecular perturbations at GW 13 offers a strategic window for intervention before the clinical onset of PE symptoms, typically occurring later in the second or third trimester. Moreover, the identification of potential biomarkers, including MYZAP, CAV2, OXTR, and GBP1, provides a foundation for developing non-invasive screening tools using maternal plasma cfRNA profiles.

4.2. Apoptosis and cellular stress

The significant enrichment of the Apoptosis and Lysosome pathways aligns with known disruptions in trophoblast turnover and placental homeostasis in PE [14]. Excessive trophoblast apoptosis can result in the release of pro-inflammatory debris into maternal circulation, further amplifying immune activation. Moreover, the involvement of mitochondrial-related processes, such as mitochondrial gene expression and rRNA processing, points to cellular stress responses that may contribute to placental insufficiency [15].

4.3. Non-coding RNAs as regulatory hubs

Non-coding RNAs (ncRNAs), particularly long non-coding RNAs (lncRNAs) and small nucleolar RNAs (snoRNAs), are central regulators of gene expression and immune responses in pregnancy. In PE, our analyses identify ncRNAs as key components of the dysregulated molecular landscape. GO enrichment highlights their role in immune modulation, including complement activation, microRNA catabolism, and regulation of inflammatory responses. These findings align with prior studies showing that lncRNAs orchestrate immune tolerance at the maternal–foetal interface and modulate trophoblast invasion, processes impaired in PE [16,17].

snoRNAs were significantly enriched in cancer-associated pathways, such as PI3K–Akt signalling and MicroRNAs in cancer. Rather than implying a neoplastic process, this overlap highlights shared molecular mechanisms between oncogenic biology and placental development, particularly angiogenesis, immune modulation, and cellular stress responses [18,19].

4.4. Comparison with the original source studies (GSE154377 and GSE192902)

Moufarrej et al. [7], using the GSE192902 dataset, demonstrated that cfRNA from maternal plasma can predict PE weeks before clinical diagnosis, primarily identifying immune and placental signalling transcripts. Del Vecchio et al. [8], using the GSE154377 dataset, focused on cfRNA and methylation signatures in pregnancies with adverse outcomes, identifying broad transcriptomic perturbations. The present study extends these findings in several important ways: (i) we perform the first gestational-week-resolved DEG analysis spanning GW 8–16 across both datasets simultaneously, enabled by cross-dataset batch correction; (ii) we specifically identify GW 13 as a prominent gestational window of transcriptomic disruption through formal cross-week comparison ($\chi^2 = 148.3$, $p < 0.001$), which neither original study addressed; (iii) we provide a comprehensive characterisation of non-coding RNA subtypes (lncRNAs, snoRNAs, pseudogenes) at GW 13, extending beyond protein-coding gene analyses in the original reports; and (iv) we integrate KEGG and GO enrichment analyses that reveal convergent immune dysregulation, apoptosis, and mitochondrial stress pathways, providing mechanistic context not explored in either original dataset publication.

4.5. Potential biomarkers and clinical implications

Several DEGs identified in this study, including MYZAP, CAV2, OXTR, and GBP1, may serve as early PE biomarkers. MYZAP, involved in cell-cell junction integrity, may indicate placental barrier disruption, while GBP1 aligns with PE's inflammatory milieu [20]. Dysregulated OXTR may contribute to placental and vascular dysfunction, and elevated first-trimester oxytocin (OXT) levels are promising for early detection although this requires confirmation in independent and later-gestation cohorts. CAV2 may affect PE indirectly via endothelial

function.

The identification of gestational week 13 as a critical window for molecular perturbation underscores the importance of early screening. Integrating cfRNA profiling into routine prenatal care could enable earlier detection of at-risk pregnancies, improving maternal and foetal outcomes.

The marked concentration of differential expression at GW 13, together with the substantially smaller number of DEGs detected in later gestational windows, suggests that the strongest transcriptomic disruption associated with PE occurs during a temporally restricted early-gestation window. However, the later-gestation analyses should be interpreted cautiously because of differences in subgroup composition and the limited number of PE and SPE samples in some windows.

4.6. Limitations and future directions

This study provides insights into the molecular landscape of PE through cfRNA profiling, highlighting potential avenues for early detection and intervention. Using publicly available datasets enabled integration of diverse sources and demonstrates the feasibility of large-scale, non-invasive molecular monitoring. Future studies with prospectively collected longitudinal data will improve understanding of dynamic gene expression across gestation.

An important limitation of the present study is the absence of genes directly associated with placental growth factor (PlGF) signalling in our DEG results. Low maternal plasma PlGF is one of the most clinically validated and widely used biomarkers for early PE screening [21]. The failure to detect PlGF-related transcripts in the cfRNA dataset may reflect several factors: cfRNA captured in maternal plasma at GW 8–16 may not yet carry sufficient placenta-derived PlGF mRNA at detectable concentrations; the datasets used (GSE154377 and GSE192902) were not specifically designed to capture angiogenic factor transcripts; or PlGF regulation may occur predominantly at the protein level or via post-transcriptional mechanisms not captured by RNA-seq. Future studies should complement cfRNA profiling with concurrent measurement of plasma PlGF protein levels to provide a more complete picture of angiogenic dysregulation in early PE.

Two further limitations concern the later-gestation and severity analyses. First, although we extended the analysis across gestation, the later windows were not designed around defined diagnostic timepoints and the number of PE cases was limited, particularly in the third trimester (27 to 39 weeks), so the absence of DEGs there should be interpreted with caution. Second, the severity comparison relied on small and uneven PE and SPE subgroups and is therefore exploratory; the inconsistent pattern across windows likely reflects these sample sizes. Prospective cohorts with balanced sampling across gestation and with graded severity and outcome data will be required to confirm both the discreteness of the GW 13 window and the severity dependence of the signal. In addition, early versus late-onset classification and maternal characteristics such as age, body mass index and parity were not available in the public metadata, so these correlations could not be performed and represent an important direction for prospectively annotated cohorts.

Combining transcriptomics with proteomics and metabolomics will enhance systems-level understanding of PE, while exploring genetic, epigenetic, and environmental interactions may support more precise, personalised maternal-foetal medicine.

5. Conclusion

This study elucidates the complex interplay between immune dysregulation, cellular stress, and non-coding RNA regulation in PE, identifying gestational week 13 as a prominent window of transcriptomic disruption associated with PE. The discovery of key pathways and potential biomarkers – such as MYZAP, CAV2, OXTR, and GBP1 – offers promising candidate avenues, pending prospective validation for early diagnosis and targeted therapeutic intervention. However, translating cfRNA profiling into routine prenatal care will require overcoming challenges related to technical variability, assay standardisation, and cost-effectiveness to ensure reproducibility and accessibility. As research advances, addressing these barriers and integrating molecular profiling into clinical workflows holds transformative potential for improving PE diagnosis, management, and pregnancy outcomes.

CRediT authorship contribution statement

Suhirthakumar Puvanendran: Writing – original draft, Visualization, Methodology, Investigation, Formal analysis, Data curation, Conceptualization. **Obed Brew:** Writing – review & editing, Supervision, Funding acquisition.

Ethics declaration

The authors have NOT obtained informed consent from participants or their legal representatives. This work is a retrospective secondary analysis of fully de-identified, publicly available cfRNA transcriptomic datasets deposited in the Gene Expression Omnibus (GSE154377 and GSE192902) under open-access terms equivalent to a Creative Commons Zero (CC0) licence. The authors had no contact with any participant and no access to identifiable personal, clinical or contact information, and no attempt was made to re-identify any individual. Informed consent for participation, and for the deposition and onward secondary use of the resulting data, was obtained by the investigators of the original studies, who also secured the relevant ethical approvals prior to public release. Seeking additional consent from these participants was therefore neither required nor feasible, as the authors have no means of contacting them. Appropriate protocols for protecting the rights and privacy of participants were observed throughout the analysis: no names, initials, hospital or other record numbers, dates of birth or other identifying details appear in this article or its supplementary materials, and all results are reported at group level, so no individual participant is identifiable from any figure, table or supplementary file.

This study was performed in compliance with relevant laws, regulatory frameworks and guidelines where the research took place. Ethics committee approval was not required under relevant laws and institutional guidelines. This study is a retrospective bioinformatics analysis of publicly available, fully de-identified transcriptomic datasets obtained from the Gene Expression Omnibus (GSE154377 and GSE192902). The research involved no direct interaction with human participants and no access to identifiable personal information, so it did not constitute human subjects research requiring institutional review board or research ethics committee review. The primary investigators of the original studies obtained the necessary ethical approvals and participant consent prior to public deposition of the data.

Funding

This research was supported by the Gates Foundation (INV-064516) through the Science for Africa Foundation (SFA) under the AI Grand Challenges initiative [Grant ID: SFA-R15-126]. The funders had no role in the study design, data collection and analysis, decision to publish, or preparation of the manuscript.

Declaration of competing Interest

The authors declare that they have no known competing financial interests or personal relationships that could have appeared to influence the work reported in this paper.

Appendix A. Supplementary data

Supplementary data to this article can be found online at https://doi.

org/10.1016/j.placenta.2026.09.008.

Data availability

The datasets analysed during this study are publicly available in the Gene Expression Omnibus (GEO) under accession numbers GSE154377 (https://www.ncbi.nlm.nih.gov/geo/query/acc.cgi?acc=GSE154377) and GSE192902 (https://www.ncbi.nlm.nih.gov/geo/query/acc.cgi?acc=GSE192902). All datasets are publicly available in GEO under open-access terms equivalent to a Creative Commons Zero (CC0) licence.

References

[1] S. Sun, W. Li, X. Zhang, A.U.R. Aziz, N. Zhang, Trends in global and regional incidence and prevalence of hypertensive disorders in pregnancy (1990–2021): an age–period–cohort analysis, Sci. Rep. 15 (2025) 1513, https://doi.org/10.1038/s41598-025-85819-0.

[2] A. Arechvo, A. Wright, A. Syngelaki, P. von Dadelszen, L.A. Magee, R. Akolekar, et al., Incidence of pre-eclampsia: effect of deprivation, Ultrasound Obstet. Gynecol. 61 (1) (2023) 26–32, https://doi.org/10.1002/uog.26084.

[3] R. Pijnenborg, L. Vercruysse, M. Hanssens, The uterine spiral arteries in human pregnancy: facts and controversies, Placenta 27 (9–10) (2006) 939–958, https://doi.org/10.1016/j.placenta.2005.12.006.

[4] G.J. Burton, C.W. Redman, J.M. Roberts, A. Moffett, Pre-eclampsia: pathophysiology and clinical implications, BMJ 366 (2019) l2381, https://doi.org/10.1136/bmj.l2381.

[5] R.J. Levine, S.E. Maynard, C. Qian, K.H. Lim, L.J. England, K.F. Yu, et al., Circulating angiogenic factors and the risk of preeclampsia, N. Engl. J. Med. 350 (7) (2004) 672–683, https://doi.org/10.1056/NEJMoa031884.

[6] J. Villar, S. Ariff, R.B. Gunier, R. Thiruvengadam, S. Rauch, A. Kholin, et al., Maternal and neonatal morbidity and mortality among pregnant women with and without COVID-19 infection: the INTERCOVID multinational cohort study, JAMA Pediatr. 175 (8) (2021) 817–826, https://doi.org/10.1001/jamapediatrics.2021.1050.

[7] M.N. Moufarrej, S.K. Vorperian, R.J. Wong, A.A. Campos, C.C. Quaintance, R.V. Sit, et al., Early prediction of preeclampsia in pregnancy with cell-free RNA, Nature 602 (7898) (2022) 689–694, https://doi.org/10.1038/s41586-022-04410-z.

[8] G. Del Vecchio, Q. Li, W. Li, S. Thamotharan, A. Tosevska, M. Morselli, et al., Cell-free DNA methylation and transcriptomic signature prediction of pregnancies with adverse outcomes, Epigenetics 16 (6) (2021) 642–661, https://doi.org/10.1080/15592294.2020.1816774.

[9] O. Brew, M.H.F. Sullivan, A. Woodman, Comparison of normal and pre-eclamptic placental gene expression: a systematic review with meta-analysis, PLoS One 11 (8) (2016) e0161504, https://doi.org/10.1371/journal.pone.0161504.

[10] D.A. Enquobahrie, M. Meller, K. Rice, B.M. Psaty, D.S. Siscovick, M.A. Williams, Differential placental gene expression in preeclampsia, Am. J. Obstet. Gynecol. 199 (5) (2008), https://doi.org/10.1016/j.ajog.2008.04.020, 566.e1–11.

[11] S. Zhang, K. Amahong, Y. Zhang, X. Hu, S. Huang, M. Lu, et al., RNAenrich: a web server for non-coding RNA enrichment, Bioinformatics 39 (5) (2023) btad421, https://doi.org/10.1093/bioinformatics/btad421.

[12] M. Michalczyk, A. Celewicz, M. Celewicz, P. Woźniakowska-Gondek, R. Rzepka, The role of inflammation in the pathogenesis of preeclampsia, Mediat. Inflamm. 2020 (2020) 3864941, https://doi.org/10.1155/2020/3864941.

[13] K. Motomura, H. Morita, K. Naruse, H. Saito, K. Matsumoto, Implication of viruses in the etiology of preeclampsia, Am. J. Reprod. Immunol. 91 (5) (2024) e13844, https://doi.org/10.1111/aji.13844.

[14] B. Huppertz, Placental origins of preeclampsia: challenging the current hypothesis, Hypertension 51 (4) (2008) 970–975, https://doi.org/10.1161/HYPERTENSIONAHA.107.107607.

[15] P. Vangrieken, S. Al-Nasiry, A. Bast, P.A. Leermakers, C.B. Tulen, P.M. Schiffers, et al., Placental mitochondrial abnormalities in preeclampsia, Reprod. Sci. 28 (8) (2021) 2186–2199, https://doi.org/10.1007/s43032-021-00464-y.

[16] S. Kannampuzha, M. Ravichandran, A.G. Mukherjee, U.R. Wanjari, K. Renu, B. Vellingiri, et al., The mechanism of action of non-coding RNAs in placental disorders, Biomed. Pharmacother. 156 (2022) 113964, https://doi.org/10.1016/j.biopha.2022.113964.

[17] A. Cerillo, R. Molitierno, P. De Franciscis, D.D. Nunziata, M. Fordellone, C. Capristo, et al., The role of lncRNAs in complicated pregnancy: a systematic review, Genes 16 (8) (2025) 959, https://doi.org/10.3390/genes16080959.

[18] MdMS. Oliveira, CdM. Salgado, L.R. Viana, M.C.C. Gomes-Marcondes, Pregnancy and cancer: cellular biology and mechanisms affecting the placenta, Cancers (Basel) 13 (7) (2021) 1667, https://doi.org/10.3390/cancers13071667.

[19] H. Pang, D. Lei, Y. Guo, Y. Yu, T. Liu, Y. Liu, et al., Three categories of similarities between the placenta and cancer that can aid cancer treatment: cells, the microenvironment, and metabolites, Front. Oncol. 12 (2022) 977618, https://doi.org/10.3389/fonc.2022.977618.

[20] J.H. Schuitemaker, R.H. Beernink, T.I. Cremers, S.A. Scherjon, M.G. Van Pampus, M.M. Faas, Healthy and preeclamptic pregnancies show differences in guanylate-binding Protein-1 plasma levels, Pregnancy Hypertens. 25 (2021) 18–24, https://doi.org/10.1016/j.preghy.2021.05.008.

[21] T.M. MacDonald, S.P. Walker, N.J. Hannan, S. Tong, T.J. Kaitu'u-Lino, Clinical tools and biomarkers to predict preeclampsia, EBioMedicine 75 (2021) 103780, https://doi.org/10.1016/j.ebiom.2021.103780.